Long-range attraction between colloidal spheres at the air-water interface: The consequence of an irregular meniscus

Dimitris Stamou and Claus Duschl
Laboratoire de Chimie Physique des Polymères et Membranes, Swiss Federal Institute of Technology, CH-1015 Lausanne, Switzerland

Diethelm Johannsmann*
Max-Planck-Institute for Polymer Research, Ackermannweg 10, 55128 Mainz, Germany
(Received 23 December 1999)

Recent observations of charged colloidal particles trapped at the air-water interface revealed long-range interparticle attractive forces, not accounted for by the standard theories of colloidal interactions. We propose a mechanism for attraction which is based on nonuniform wetting causing an irregular shape of the particle meniscus. The excess water surface area created by these distortions can be minimized when two adjacent particles assume an optimum relative orientation and distance. Typically, for spheres with diameter of 1 μm at an interparticle distance of 2 μm, deviations from the ideal contact line by as little as 50 nm result in an interaction energy of the order of $10^4 kT$. Roughness-induced capillarity explains the experimental findings, including the cluster dissolution caused by addition of detergent to the subphase and the formation of linear aggregates. This kind of interaction should also be of importance in particle-stabilized foams and emulsions.

PACS number(s): 82.70.Dd, 68.70.+w, 05.40.−a

I. INTRODUCTION

The lateral organization of colloidal particles at gas-liquid interfaces is of interest for a number of different reasons. On the side of fundamental physics, it sheds light on the influence of dimensionality on the phase behavior [1], Pieranski was the first to demonstrate the formation of two-dimensional crystals from charged colloids at the air-water interface [2]. More recently, other authors used monolayers of magnetic colloids to demonstrate a transition from a two-dimensional (2D) liquid to a 2D solid phase via defect unbinding according to the Kosterlitz-Thouless mechanism [3,4]. On the practical side, 2D colloidal arrays have been used as templates for nanostructuring solid surfaces [5,6]. Fendler reviewed the use of nanoparticles assembled at the water surface and transferred to solid supports for the formation of electronic and electrooptic devices [7]. The formation of 2D particle arrays through dewetting processes was extensively investigated for its relevance for 2D protein crystallization [8]. The organization of particles at interfaces is also of significance for a number of industrial applications [9]. Inclusion of particles in a suspension is a method for stabilizing and refining the properties of emulsions and foams [10,11]. Such particles, trapped at a two-phase boundary, will also be subject to the kind of capillary force described here.

In all these examples, knowledge of the different contributions that shape the particle interaction potential is critical. In 1997 an unexpected attractive interaction was found by the authors of Ref. [12], independently confirmed by Ghezzi and Earnshaw [13] and ourselves [5]. The system in question was an assembly of negatively charged (sulphate) polystyrene particles 0.5–5 μm in diameter spread at the air-water interface. They were found to associate in clusters with interparticle distances that were several times their diameter [14–16]. A synopsis of the known pairwise attractive interactions illustrates that none of them can produce a minimum in the interaction potential at micrometer distances.

(i) Two-dimensional aggregation of uncharged colloid particles at the air-water interface was frequently observed [17]. This is in all likelihood caused by the van der Waals attraction [18]. Even for charged colloids van der Waals aggregates occur if the electrostatic repulsion is screened by sufficient amounts of salt in the subphase [19–21]. However, at distances above one micrometer the van der Waals energy, E_{vdW} between two spheres is much smaller than the thermal energy kT [13]. As a first approximation [22] one has $E_{\mathrm{vdW}} = AR/(12D)$, with A the Hamaker constant and D the separation between the particle surfaces. For spheres partly immersed in water the effective Hamaker constant has a value between $A = 6.6 \times 10^{-20}$ J (in air) and $A = 10^{-20}$ J (in water). By inserting $R = 0.5\,\mu$m and $D = 1\,\mu$m, one arrives at $E_{\mathrm{vdW}} \approx (0.1-0.6)kT$.

(ii) An attraction between particles floating on a liquid surface mediated by gravity was previously described by Chang, Henry, and White [23]. These authors considered spheres which were heavy enough to cause local depressions of the water surface. The overall potential energy can be decreased when two such depressions combine to form a single trough containing both particles in its center. The interaction energy is $2\pi R^6 \gamma^{-1} \rho^2 g^2 S_p^2 K_0(\lambda L)$, with R the particle radius, γ the surface tension, ρ the density of water, g the gravitational acceleration, S_p a number of order unity depending on the particle's density and contact angle, K_0 the modified Bessel function of the second kind of order zero, $\lambda = (\rho g \gamma^{-1})^{1/2}$ the

*Corresponding author. Email address: johannsmann@mpip-mainz.mpg.de

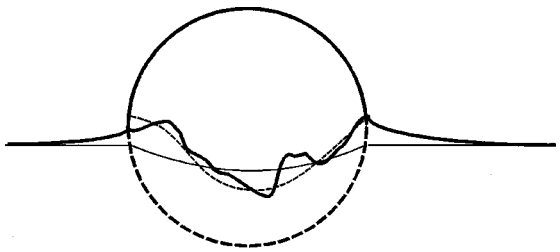

FIG. 1. Schematic description of a rugged meniscus at the particle surface. It is assumed that the meniscus is pinned to heterogeneities on the particle surface, and thereby distorts the nearby water surface. The thin straight line is the ideal contact line in the absence of pinning. The thin dashed line is an approximation of the real contact line by $h(r_c,\varphi)\approx H_2\cos[2(\varphi-\varphi_{2,0})]$. It represents the quadrupole moment of the meniscus.

inverse capillary length, and L the particle separation. The interaction scales as the square of particle mass, and therefore depends very strongly on the particle radius R. For polystyrene on water it is comparable to the thermal energy kT at a particle radius of 5 μm, and is much less than kT at $R=0.5\,\mu$m, which is the particle radius in our experiments. Capillary attraction according to Ref. [23] therefore cannot explain our findings.

(iii) Immersion capillary forces [24,25], if present in this system, would result in attractive forces sufficient to explain the observations. Since the particles are spread from methanol one could argue that a thin solvent-rich layer may remain at the water surface. On the grounds of two experimental observations (discussed in more detail below) we judge this scenario as improbable: first, the interaction can be reversibly switched off and on by addition and removal of detergent, and, second, the observed patterns of aggregation survive an exchange of the water subphase. Both of these findings are incompatible with the notion of a thin solvent film inducing aggregation.

In the following we propose a mechanism for lateral attraction which is based on distortions of the water surface caused by an irregularly shaped meniscus. It is assumed that the three-phase contact line is not straight but rather has a rugged shape because of chemical or topographical heterogeneities (Fig. 1) [26]. Pinning of a meniscus to topographic or chemical defects is well known from planar surfaces [27,28]. Interestingly, an exceptionally large contact angle hysteresis has been reported for polystyrene surfaces by Good and Kotsidas [29]. An unevenly pinned meniscus will distort the water surface. When two particles come close to each other there will be a favorable relative orientation, where the integral excess area—and hence the surface energy—is minimized (Fig. 2). The depth of this minimum is a function of *particle distance*, resulting in a lateral force. On the macroscopic scale such a phenomenon can be readily observed when spreading corn flakes on a water surface. Nonuniform wetting rotates these macroscopic objects around, and pulls them together into chains and rafts.

The experimental observation of the particles at the air-water interface was conducted with fluorescence microscopy (Fig. 3). Inspection of the two-dimensional layer in all cases revealed particles in clusters with interparticle separations of at least twice the particle diameter of 1 μm. Detergent was added to the subphase, modifying the particle surface properties. The aggregation patterns change gradually with the concentration of detergent. In Sec. III we elaborate on the observations, and discuss the different ways in which the presence of detergent can modify the interaction. We then develop the theory to describe the capillary interaction between two particles as a function of relative orientation and distance. We conclude with a comparison between observation and the predictions arising from the treatment of the nonuniform wetting concept.

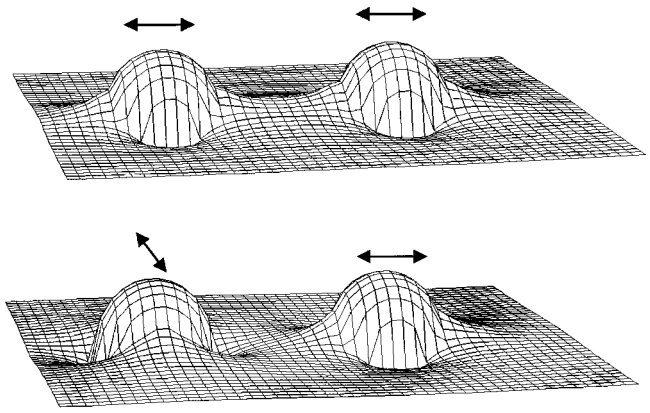

FIG. 2. Height of the water surface around two interacting particles. The meniscus has a quadrupolar distortion, that is, the three-phase line follows the law $h(\varphi)=H_2\cos[2(\varphi-\varphi_{2,0})]$, with H_2 an amplitude, φ the azimuthal angle, and the $\varphi_{2,0}$ the orientation of the particle. In case (a) the particles are oriented parallel, that is, the sides with the meniscus higher than average face each other. In between these particles the slope of the water level is *reduced*, when the particles approach each other, resulting in a gain in surface energy. With particles oriented perpendicular to each other (b) the slope is *increased*, resulting in energy penalty upon approach.

II. MATERIALS AND EXPERIMENTAL TECHNIQUES

In the set of results presented here we used polystyrene microspheres (molecular probes) with a diameter of 1.06 μm $\pm 2\%$. They were fluorescently labeled. According to the manufacturer, the particles are prepared by a surfactant-free process, and electrostatically stabilized against aggregation by a high density (8.5 μC/cm^2) of sulfate (SO_4^-) surface charges. The product was delivered as a suspension (2 wt %) in 2-mM sodium azide, the latter compound being added to prevent bacterial growth. Prior to experiment the particles were further dialyzed to remove sodium azide and any ion-polymer traces. A Slide-A-Lyzer (Pierce) with a 10 000-MW cutoff membrane was used as a dialysis chamber. A volume of 0.5 ml of 2-wt % solution was dialyzed against 1 L of a 10-mM ethylenechiaminetetraacetic acid (EDTA) solution for the first day, and deionized water (specific resistance 18 MΩ cm, Millipore) for another six days. The temperature was always kept at 60 °C. From the recovered material 0.1-wt % solutions in MeOH/water 9/1 were prepared and applied to the water surface as such.

The experiments at the air-water interface were performed on a commercial Langmuir trough (Riegler & Kirstein) which was mounted on an *xyz* stepper-motor driven translation stage (Märzhauser). Immediately after spreading one could find the majority of the particles trapped irreversibly at the interface. The evolution of the monolayers was moni-

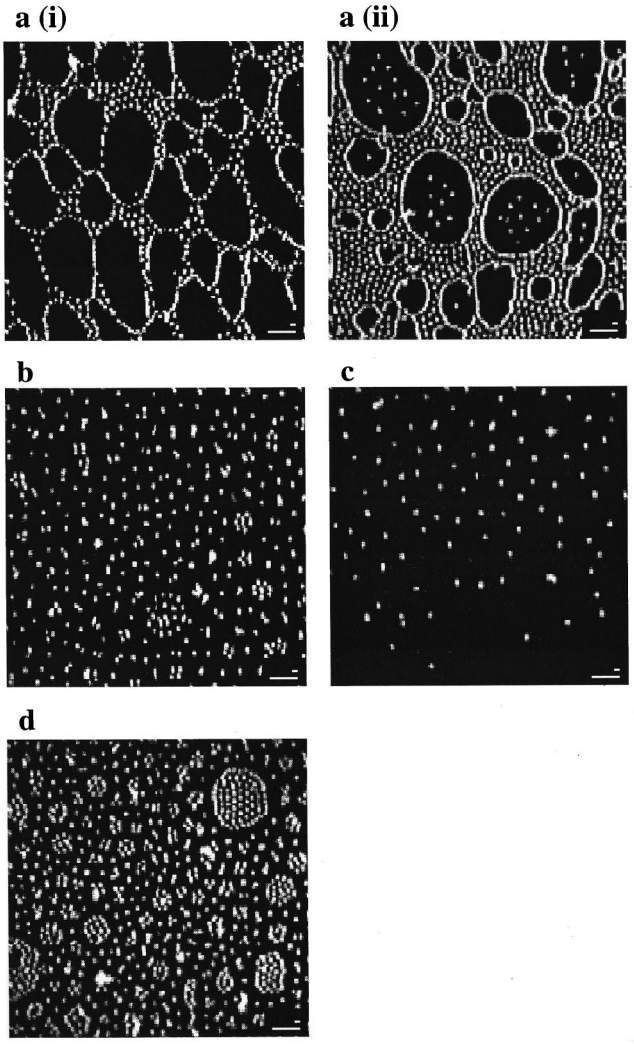

FIG. 3. Fluorescence micrographs of the particle distribution at the air-water interface. The particle diameter is 1 μm. Scale bars are 2 and 10 μm. Note that the particles appear larger than they are due to camera gain saturation. This gives the impression that some particles touch each other. Conversely, they actually never do (with the exception of few isolated van der Waals pairs). (a) (i) and (a) (ii). Configurations after spreading. One sees many strings. The smallest interparticle distance is 2 ± 0.5 μm. (b) After addition of 40 μM of detergent, one finds a rather broad distribution of cluster sizes. (c) At a detergent concentration of 70 μM, the attractive force is still present. However, the average interparticle distance has increased to 10 ± 3 μm. (d) After purging with detergent free water, the clusters reappear but are somewhat looser now.

tored with a Zeiss Axiotron microscope in epifluorescence. Images were recorded with a video camera (Hamamatsu), and stored on videotape. Due to the strong fluorescence of the particles the camera recorded them larger than they actually are. Because of this artifact, Fig. 3 suggests that in some cases the aggregated particles touch each other. Conversely, the particle distance in closest approach is about 2 μm which is twice the particle diameter [see Fig. 3(a)].

The particles were always spread on detergent-free water. NaCl (1 mM) was added to the subphase in order to achieve a well-defined electrostatic screening length [22] of $\kappa^{-1/2} \approx 9.5$ nm. Octylglucoside (*n*-octyl-β-D-glucopyranoside, Alexis Co.), was introduced later either by injection of concentrated solutions or by slow exchange of the subphase with a solution of the desired concentration. The latter was achieved with an inlet and an outlet behind the two barriers. Final detergent concentrations varied from 5 μM to 10 mM.

III. PHENOMENOLOGY OF PARTICLE AGGREGATION

Figure 3 shows representative images of the different states of aggregation. Immediately after spreading [Figs. 3(a)(i) and 3(a)(ii)], the particles are strongly clustered. One finds many linear strings, indicative of an anisotropic interaction [16]. Clearly, the interaction potential has a minimum at an interparticle distance of a few micrometers. Such a minimum requires a long-range attraction compensating the repulsive dipole-dipole interaction of the charged spheres [27,28].

We propose that minute deviations ($\approx$10 nm) of the meniscus from the ideal, straight three-phase contact line can produce such attractive forces. To substantiate this argument we sought experimental means of modifying the particles at the air-water interface in a way that would affect contact angle hysteresis and pinning [27,28] but not the other system parameters. For that purpose we introduced detergent in the subphase. Detergent molecules will absorb on the surface of a particle, expose hydrophilic headgroups toward water, and thus alter its surface properties. Octylglucoside was considered the most appropriate detergent for two reasons. First, it is neutral and will hence not affect the charge of the particles. Second, it is easily back-exchanged by renewal of the water subphase due to its high critical micellar concentration of 23 mM [30]. Partial dialysis of the absorbed detergent allows for monitoring the effect it has on particle aggregation in a reversible manner. Interestingly, the detergent concentrations required to change the interparticle distances were so low that the air-water surface tension was not changed by more than 1 mN/m. This suggests that the variations in the aggregate morphology do not come about by a change in surface tension, but rather by a change in the contact angle due to adsorption of detergent to the particle surfaces.

As shown in Fig. 3(f), addition of 40-μM octylglucoside initiates cluster dissociation. Still, there is a rather broad size distribution of clusters that are stable over several hours. At 70-μM octylglucoside [Fig. 3(c)], the majority of clusters has gone through a ''phase transition,'' and now have a much increased average interparticle separation. At first, the clusters appear to have dissolved and form a homogeneous layer. This, however, is not the case. Allowing space (and time) for the monolayer to expand reveals a new equilibrium distance of 10 ± 3 μm. As Fig. 3(c) shows, there are boundaries separating the domains with the new, larger particle distance from areas which are almost empty. If the surface area is not large enough the new, low-density domain completely fills the trough. In this case the long-range attraction is easily missed. Further increase of the detergent concentration (results not presented) did not further change the picture.

Figure 3(d) depicts the monolayer after extensive purging ($>10\times$subphase volume) with detergent-free water. We expect most but not all of the absorbed detergent to be removed from the particle surface. Aggregates have formed again. There is an ''edge effect'' in the sense that the particles at

the domain boundaries are closer to each other than the particles in the center. The same edge effect was already seen immediately after spreading. Also note that the particles are depleted immediately outside of the domains boundaries, indicative of a long-range repulsive interaction. Upon repeated addition and removal of detergent, states (c) and (d) disappear and reappear in a fully reversible way. However, the state found right after spreading is not recovered. Probably, the initial structure of the system is to some extent affected by the rather turbulent spreading process. Also, some of the strings seen in Fig. 3(a) may have irreversibly ruptured by the addition of detergent.

IV. THEORY

In this section we calculate of the interaction energy δE_{AB} between two particles as a function of their relative orientation and separation. From our point of view the dependence of the attraction on the detergent concentration proves that surface tension must be somehow part of the picture. The proposed mechanism is based on distortions of the water surface caused by nonuniform wetting. Interactions of this kind have been discussed in the literature by different authors but have never been explicitly put into the context of 2D colloidal aggregates [31–33]. We first derive an expression for the height of the water surface around an isolated particle. This is then translated to an excess area δS created at the air-water interface. The energy cost per particle is simply $\delta E = \gamma \delta S$, where γ is the air-water surface tension. In a second step, we derive an approximation of the excess area around two interacting particles A and B. Knowing the single particle term one can calculate the interaction energy as $\delta E_{AB} \approx \gamma(\delta S_{AB} - \delta S_A - \delta S_B)$ [see Eq. (18)].

Since all length scales are below the capillary length of $\lambda^{-1} = 2.7\,\mathrm{mm}$, effects of gravity may be ignored, and the pressure drop across the water surface is zero. According to the Young-Laplace equation [34] this implies that the mean curvature of the water surface vanishes everywhere. We assume that the slope of the water surface is small everywhere ($\ll 45°$), and we therefore approximate the mean curvature by $\Delta h(r,\varphi)$ with Δ the Laplace operator and $h(r,\varphi)$ the local water level. In the following we use cylinder coordinates r and φ centered around the sphere. According to the Young-Laplace equation we have

$$\Delta h(r,\varphi) = \left(\frac{1}{r}\frac{\partial}{\partial r} r \frac{\partial}{\partial r} + \frac{1}{r^2}\frac{\partial^2}{\partial \varphi^2} \right) h(r,\varphi) = 0. \tag{1}$$

There is a certain analogy with 2D electrostatics, where h takes the role of a potential and a rough meniscus corresponds to a charge distribution. To solve the Young-Laplace equation we write the function $h(r,\varphi)$ as a product,

$$h(r,\varphi) = R(r)\Phi(\varphi), \tag{2}$$

where the functions $R(r)$ and $\Phi(\varphi)$ only depend on r and φ, respectively. The Young-Laplace equation then reads

$$0 = \left(\frac{1}{r}\frac{\partial}{\partial r} r \frac{\partial}{\partial r} R(r) \right) \Phi(\varphi) + \left(\frac{1}{r^2}\frac{\partial^2}{\partial \varphi^2}\Phi(\varphi) \right) R(r), \tag{3a}$$

or, equivalently,

$$\frac{1}{R(r)} \left(r \frac{\partial}{\partial r} r \frac{\partial}{\partial r} R(r) \right) = -\frac{1}{\Phi(\varphi)} \left(\frac{\partial^2}{\partial \varphi^2}\Phi(\varphi) \right). \tag{3b}$$

Equation (3b) holds for all values of r and φ independently. Therefore, the expressions on the left- and right-hand-sides must both be constant. We term the separation constant m^2. It will turn out that m is an integer, and labels the different modes. The modes are the orders of a multipole expansion. Equations (3) then read as

$$\frac{\partial^2}{\partial \varphi^2}\Phi_m(\varphi) = -m^2 \Phi_m(\varphi), \tag{4a}$$

$$r\frac{\partial}{\partial r} r \frac{\partial}{\partial r} R_m(r) = m^2 R_m(r), \tag{4b}$$

which are fulfilled by the functions

$$\Phi_m(\varphi) = \Phi_{m,0}\cos(m(\varphi - \varphi_{m,0})), \tag{5a}$$

$$R_m(r) = R_{m,0} r^{-m}. \tag{5b}$$

The coefficients $R_{m,0}$, $\Phi_{m,0}$, and $\varphi_{m,0}$ follow from the boundary conditions. The sphere and the water surface intersect at the contact radius r_c which is close to the particle radius R unless the contact angle is very low or very high. We decompose the height of line $h(r_c,\varphi)$ into multipoles according to

$$h(r_c,\varphi) = \sum_{m=2}^{\infty} H_m \cos(m(\varphi - \varphi_{m,0})), \tag{6}$$

with expansion coefficients H_m and phase angles $\varphi_{m,0}$. The prefactor H_m is equal to $R_{m,0} r_c^{-m} \Phi_{m,0}$. Monopoles ($m=0$) are forbidden because there is no external force like gravity dragging the particles away from their optimum height. In fact, for heavy enough particles the monopole term becomes allowed, and our formalism reduces to the result of Ref. [23]. The dipole term ($m=1$), is forbidden because there is no external torque rotating the particles away from their optimum orientation relative to the water surface [35]. This leaves the quadrupole term $m=2$ as the lowest allowed multipole order.

Equation (5b) states that the different multipole orders decay with an inverse power equal to the multipole order. The quadrupole order is the lowest allowed order and decays as r^{-2}. For a long-range interaction the quadrupole term is the most important one. We therefore confine ourselves to the quadrupole term in the following. It is given by

$$h^{(2)}(r,\varphi) = H_2 \cos[2(\varphi - \varphi_{2,0})] \left(\frac{r_c}{r} \right)^2, \tag{7}$$

where the prefactor H_2 gives the height of the meniscus at the contact line.

We now calculate the ''self-energy'' of an individual particle. It is equal to the excess area times the surface energy. The excess area δS is the difference between the surface area S^* and the projected surface area S. First we consider an infinitesimal element $dS^* = dx^* \times dy^*$. We use a local co-

ordinate system rotated such that the slope is a maximum along the y coordinate, that is, $dx = dx^*$. For dy^* we find

$$\begin{aligned} dy^* &= \sqrt{dy^2 + dh^2} \\ &\approx \left[dy^2 + \left(\frac{dh}{dy} \right)^2 dy^2 \right]^{1/2} \\ &= dy \sqrt{1 + (\nabla h)^2} \\ &\approx dy \left(1 + \frac{1}{2} (\nabla h)^2 \right), \end{aligned} \tag{8}$$

resulting in

$$\delta(dS) = dS^* - dS = dx\, dy\, \tfrac{1}{2} (\nabla h)^2 \tag{9}$$

or

$$\delta S = \tfrac{1}{2} \int_{r=r_c}^{\infty} \int_{\varphi=0}^{2\pi} (\nabla h)^2 r\, d\varphi\, dr. \tag{10}$$

In the quadrupole approximation, one has

$$\begin{aligned} \nabla h \cdot \nabla h &\approx \left(\frac{\partial}{\partial r} h^{(2)} \right)^2 + \frac{1}{r^2} \left(\frac{\partial}{\partial \varphi} h^{(2)} \right)^2 \\ &= 4 H_2^2 r_c^4 r^{-6}. \end{aligned} \tag{11}$$

The self-energy $\delta E = \gamma \delta S$ is

$$\begin{aligned} \delta E &\approx 2 \gamma H_2^2 r_c^4 2\pi \int_{r=r_c}^{\infty} r^{-6} r dr \\ &= \pi \gamma H_2^2. \end{aligned} \tag{12}$$

The prefactor H_2 can be estimated from typical values of contact angle hysteresis, which we here choose as $\Delta\theta = 10°$. A typical value for pinning-induced deviations from the ideal contact line is $H_2 \approx \frac{1}{2} R \times \Delta\theta \approx 50\,\mathrm{nm}$, which is about 10% of the particle radius. With these input parameters, the self energy δE comes out to be $\delta E \approx 4\, 10^{-16}\,\mathrm{J} \approx 10^5 \mathrm{kT}$.

In a second step we calculate the interaction between two particles with a center-of-mass separation L. The interaction energy δE_{AB} is given by

$$\delta E_{AB} = \gamma (\delta S_{AB} - \delta S_A - \delta S_B), \tag{13}$$

with δS_{AB} the surface area around the interacting particles, and δS_A and δS_B the surface area around the isolated particles. In the following we make use of the ''superposition approximation'' [23]. We consider potential fields h_A and h_B emanating from hypothetical isolated particles A and B. For interacting particles the boundary conditions at the particle surfaces would have to be fulfilled not just by these fields emanating from the individual particles, but by the total field around the interacting particles. This is a rather complicated problem. We assume that the field h_A is small at particle B, and vice versa. Then the inverse power laws from Eq. (7) match the boundary conditions and the total field h_{AB} is just the sum $h_A + h_B$. Inserting Eq. (10) into Eq. (13) yields.

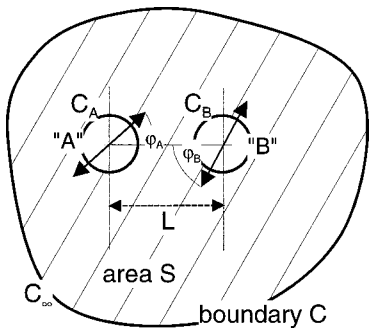

FIG. 4. Sketch of the geometry and some variables. By virtue of the first Green identity the integral over the area S is transformed into an integral over the boundary C. Since the integrand vanishes at infinity, only the lines C_A and C_B have to be evaluated.

$$\begin{aligned} \delta E_{AB} &= \frac{\gamma}{2} \int (\nabla (h_A + h_B))^2 - (\nabla h_A)^2 - (\nabla h_B)^2 dS \\ &= \gamma \int \nabla h_A \cdot \nabla h_B\, dS. \end{aligned} \tag{14}$$

The integral over the area can be transformed into an integral over the boundary by the first Green identity [8,36]

$$\int_S \nabla h_B \cdot \nabla h_A\, dS = \int_C h_B (\mathbf{n} \cdot \nabla h_A) dC - \int_S h_B \Delta h_A\, dS, \tag{15}$$

where S is the area and C is the boundary. We illustrate the geometry and the definition of some variables in Fig. 4. The boundary C consists of three closed curves, which are C_∞ at infinity and C_A and C_B at the meniscus of the particles. $\mathbf{n}$ is a unit vector perpendicular to the boundary pointing away from the area of integration. The second term on the right-hand side of Eq. (15) is zero according to the Young-Laplace equation.

With the Green identity the integral over the area was transformed into an integral over a line. Since the integrand falls off as r^{-5} as $r \to \infty$, the line integral over the outer border C_∞ is zero. Only the boundaries of the particles C_A and C_B remain. Assuming for simplicity that the two particles have the same quadrupole H_2 moment, it is enough to consider only C_B and multiply by 2 to account for C_A. Assuming that the distance L is much larger than the radius r_c one can Taylor expand the field ∇h_A at C_B as

$$\begin{aligned} \nabla h_A(\mathbf{r}) &\approx \nabla h_A(0) + \mathbf{r} \cdot (\nabla \otimes \nabla) h_A(\mathbf{0}) \\ &\approx H_2 r_c^2 \begin{pmatrix} -\dfrac{2\cos(2\varphi_A)}{L^3} + \dfrac{6r\cos(\varphi + 2\varphi_A)}{L^4} \\ \dfrac{2\sin(2\varphi_A)}{L^3} - \dfrac{6r\sin(\varphi + 2\varphi_A)}{L^4} \end{pmatrix}, \end{aligned} \tag{16}$$

where bold symbols indicate vectors, $\otimes$ is the outer product, and φ_A and φ_B are the orientations of particles A and B (Fig. 4). The angles φ_A and φ_B are defined relative to the line joining the particles (the ''bond''). We have chosen a local coordinate system (r, φ) centered at particle B. In this coor-

dinate system, particle A is located at (L,π). With this Taylor approximation the integral from Eq. (15) over the line C_B is

$$\begin{aligned}\int_{C_B} h_B(\mathbf{n}\cdot\boldsymbol{\nabla}h_A)dC &= H_2^2 r_c^2 \int_D^{2\pi} \cos[2(\varphi-\varphi_B)]\begin{pmatrix}-\cos(\varphi)\\-\sin(\varphi)\end{pmatrix} \\ &\times\begin{pmatrix}\dfrac{-2\cos(2\varphi_A)}{L^3}+\dfrac{6r_c\cos(\varphi+2\varphi_A)}{L^4}\\ \dfrac{2\sin(2\varphi_A)}{L^3}-\dfrac{6r_c\sin(\varphi+2\varphi_A)}{L^4}\end{pmatrix} r_c\,d\varphi \\ &= -6\pi H_2^2\cos[2(\varphi_A+\varphi_B)]\frac{r_c^4}{L^4}. \end{aligned} \tag{17}$$

The total interaction energy δE_{AB} is

$$\begin{aligned}\delta E_{AB} &= 2\gamma\int_{C_B} h_B(\mathbf{n}\cdot\boldsymbol{\nabla}h_A)dC \\ &= -12\pi\gamma H_2^2\cos[2(\varphi_A+\varphi_B)]\frac{r_c^4}{L^4} \\ &\approx -12\cos[2(\varphi_A+\varphi_B)]\frac{r_c^4}{L^4}\delta E. \end{aligned} \tag{18}$$

The factor of 2 in the first line accounts for the two boundaries C_A and C_B. Equation (18) is the central result of the calculation. The two particles will first rotate relative to each other until the angle-dependent prefactor is a minimum, and then be attracted to each other. The capillary interaction in quadrupolar order scales as the inverse fourth power of distance.

The interaction energy δE_{AB} may very well be much stronger than the thermal energy kT. With pinning-induced deviations from the ideal contact line of 50 nm, a particle diameter of 1 μm, and an interparticle distance of twice the particle diameter, one finds $\delta E_{AB}\sim 5\times 10^4 kT$. In order to further assess the strength of the interaction, we set δE_{AB} equal to kT, and derive the maximum separation $L_{\max}$, for which the interaction is still comparable to the thermal energy scale. Using $\delta E\approx\pi\gamma H_2^2$ [Eq. (12)], $H_2=\frac{1}{2}R\Delta\theta$, ($\Delta\theta\approx 10^\circ$ is the contact angle hysteresis), $r_c\approx R=0.5\,\mu$m, and $\varphi_A=\varphi_B=0$, we find a maximum range of $L_{\max}\approx 15\,\mu$m. A second criterion of the strength of the interaction could be the minimum size of particles which still ''feel'' the capillary attraction. Setting $L=4r_c$, $\delta E_{AB}=kT$, $r_c\sim R$, $\varphi_A=\varphi_B=0$, and $\Delta\theta=10^\circ$, we find a minimum radius of $R_{\min}\sim 7$ nm. The capillary attraction should therefore be sizable well down to the nanoscopic range.

At this point the analogy with 2D electrostatics is again helpful. Electric quadrupoles are attracted to regions with a high electric field gradient. To emphasize the analogy, we combine Eqs. (16) and (17) into the form

$$\begin{aligned}\int_{C_B} h_B(\mathbf{n}\cdot\boldsymbol{\nabla}h_A)dC &= \left\{\int_0^{2\pi} -h_B(\mathbf{r}_c)\mathbf{r}_c\,d\varphi\right\}\cdot\boldsymbol{\nabla}h_A(\mathbf{0}) \\ &+\left\{\int_0^{2\pi} -h_B(\mathbf{r}_c)\mathbf{r}_c\otimes\mathbf{r}_c\,d\varphi\right\}: \\ &\times(\boldsymbol{\nabla}\otimes\boldsymbol{\nabla})h_A(\mathbf{0}), \end{aligned} \tag{19}$$

where $\mathbf{r_c}$ is a vector of length r_c. The first and second terms in curly brackets are the dipole moment and the quadrupole moment of particle B. $(\boldsymbol{\nabla}\otimes\boldsymbol{\nabla})h_A$ is the curvature tensor of field h_A. The gradient term vanishes if the coordinate system is rotated suitably [35]. Since the dipole term vanishes, the spheres are attracted to locations of high surface curvature. This is the analog of the interaction of electric quadrupoles with gradients of the electric field. It is well known that electric quadrupoles interact with a force proportional to the inverse sixth power of distance. Note, however, that the power laws of interaction depend on dimensionality. In two dimensions the interaction between two electric charges scales the logarithm of distance, not as the inverse distance. Electric quadrupoles in two dimensions interact with a potential proportional to L^{-4}, not to L^{-5}, as in three dimensions. The same power law of L^{-4} is found for the ''capillary quadrupoles.''

Before discussing the consequences of our model, we again summarize the assumptions. These are: (a) a small slope of the water surface, (b) the neglect of multipole orders higher than $m=2$, (c) the superposition approximation, and (d) a Taylor expansion of the field emanating from one particle around the center of the other particle. The first approximation is fulfilled provided that the meniscus irregularities are small compared to the particle diameter, which seems reasonable as long as the contact angle hysteresis is not exceptionally large. The three latter approximations all require large interparticle distances.

This leaves the question of what happens at small distances. The picture is complicated because many multipole orders come into play. However, it is clear that the distance dependence of the attractive force must become weaker. As we show in the Appendix, the potential may even become repulsive at very small distances. In a situation where the attractive capillary interaction depends on distance with an inverse power of less than 3 the electrostatic dipole-dipole repulsion (scaling as L^{-3}) will sooner or later take over again. In between these regimes there is a minimum of the interaction potential defining the equilibrium distance. Although a quantitative calculation of the equilibrium distance is difficult, it is still reasonable that the assumptions used for the derivation of L^{-4} law become invalid when the interparticle distance is comparable to the particle diameter.

The overall potential between two spheres is the result of a superposition of capillarity and electrostatics. The electrostatic interaction is mainly given by a dipole-dipole repulsion, as discussed by Pieranski [2], and further elaborated by Hurd [37]. It scales as L^{-3}. The electric dipole is formed by the particle itself and a cloud of counterions located underneath it. Possibly, other Derjaguin-Landau-Verwey-Overbeek (DLVO)-like repulsive interactions also come into play when the distance between the particle surfaces is less than the Debye screening length. Figure 5 schematically de-

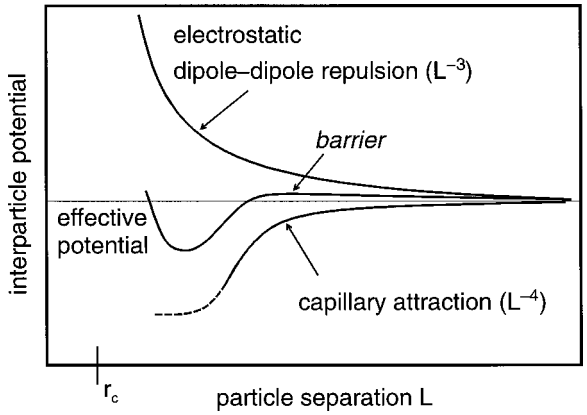

FIG. 5. Sketch of the overall potential including electrostatic contributions. For simplicity, the van der Waals minimum corresponding to particles touching each other is omitted. At large distance the electrostatic dipole-dipole repulsion scaling as L^{-3} dominates. As the particles approach each other the capillary attraction scaling as L^{-4} comes into play. There is a local maximum acting as a barrier for aggregation. At distances lower than the barrier distance the capillary attraction is strong enough to overcome the electrostatic dipole-dipole repulsion. However, when the particle distance becomes comparable to twice the particle diameter, the L^{-4} law for capillarity no longer holds and the capillary attraction levels off. Dipole-dipole repulsion again takes over.

picts the interaction potential, including capillary attraction and electrostatic repulsion. At large distances the dipole-dipole repulsion ($\propto +L^{-3}$) exceeds capillarity ($\propto -L^{-4}$), and the potential is repulsive. As the particles approach each other the relative strength of capillarity increases until it overcomes electrostatics. The maximum between the repulsive and the attractive part acts as an activation barrier for particle clustering. Finally, at a distance of about twice the particle diameter the L^{-4} law is no longer valid. The capillary attraction levels off and electrostatics again takes over. Before this happens there is a minimum in the interaction energy, which determines the two-particle distance.

The issue of anisotropy is somewhat subtle. Our experiments give evidence that there is preferential formation of strings and disordered clusters. Would an interaction like the one described here explain such an anisotropic particle association? The question can be rephrased to the following: if the orientation φ_B of particle B with respect to the bond between particles A and B is fixed, will the interaction potential with a third particle C depend on the direction of the bond between B and C? Taking Eq. (18) at face value, the answer is no. Let us say that particle C approaches the dimer from a given direction and attempts to form a bond in this same direction. The orientation of [cf. Eq. (18)] particle B relative to the new bond is fixed and given by $\varphi_B'=\varphi_B-\alpha$, where α is the angle between the two bonds. Because the interaction energy δE_{BC} depends only on the *sum* $\varphi_B'+\varphi_C'$, particle C can still find an orientation φ_C' which maximizes the attraction, regardless of the value of φ_B'. However, this picture ignores interactions at higher multipole orders. For example, the interaction between a quadrupole and a hexapole contains a term proportional to L^{-5} with a prefactor $\cos(2\varphi_B'-3\varphi_{C,3}')$ where $\varphi_{C,3}'$ is the phase angle of the hexapole of particle C. Since the interaction depends on both $(\varphi_B'+\varphi_C')$ and $(2\varphi_B'-3\varphi_{C,3}')$, it depends on φ_B' *individually*, as well. When minimizing the energy including higher multipole orders there is a dependence on the bond angle.

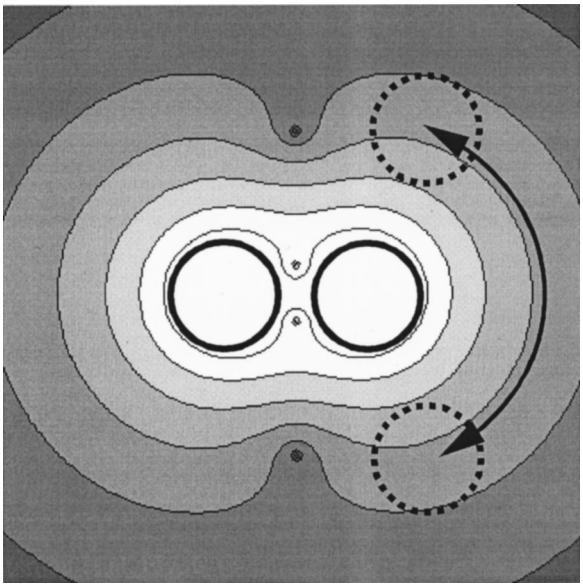

FIG. 6. Illustration of the formation of linear aggregates. The plot shows the curvature of the meniscus around two interacting particles, with minima at the sides of the pair (top and bottom part of the picture). Bright areas correspond to regions with a large difference between the eigenvalues of the curvature tensor. Since a third particle will be attracted to regions of high curvature, it will attach at the apex of the existing agglomerate, and thereby extend its length. The bond angles between successive particles in a chain should exceed 120°.

Multiparticle interactions may also lead to anisotropy. Consider, for instance, the interaction of a third particle C with the dimer A-B. Using the analogy with electrostatics, one can assume that the third particle will be attracted to regions of high local surface curvature. The latter can be numerically calculated quite easily even for complicated geometries. Figure 6 shows the results of such a calculation in a contour plot. Assuming that the third particle can only approach the dimer to a distance down to about twice the particle diameter, one sees that a third particle will probably attach at the apex of the dimer, not at its side. The region of a likely attachment is indicated with an arrow. Similar arguments were raised previously in an electrostatic context [37].

V. COMPARISON WITH EXPERIMENT

A quantitative comparison between theory and experiment would require the calculation of many-particle interactions, which is beyond the scope of this publication. Also, the input parameters of the calculation such as the shape of the meniscus, are not known and vary from particle to particle. However, some qualitative conclusions can be drawn from the two-particle interaction and compared to experiment.

(i) The shape of the meniscus is certainly different on

different particles. Some ''clean'' particles will have fewer pinning sites than others. When tuning the interaction by the addition of detergent, one expects a broad transition, where the fraction of clustered particles gradually decreases according to the distribution of heights of the meniscus irregularities. Indeed, Fig. 3(b) shows such a broad range of cluster sizes. What is not easily explained, though, is the apparent bimodal distribution of interparticle distances. As proposed by Ghezzi and co-workers, a complete description of the interaction potential may benefit from the inclusion of a more elaborate electrostatic term [38,39].

(ii) Equation (18) suggests that the strength of the interaction scales with the fourth power of the particle radius R. As a consequence, clustering should be less prominent for smaller particles. Indeed, Refs. [12] and [13] provide a critical particle size (0.95 and 0.5 μm, respectively), below which clustering is not observed. Of course this critical size is expected to depend on experimental parameters that will modify either the attractive or the repulsive contributions to the interaction potential (pretreatment, surface charge density, etc.)

(iii) The long-range repulsive electrostatic interaction [37], should result in an activation barrier for aggregation (Fig. 5). This repulsion is evidenced in experiment. Particles not connected to an aggregate are depleted around the aggregate boundaries [Fig. 3(a)(ii)].

(iv) The quadrupolar interaction is frustrated for hexagonal arrays because the optimum relative orientations cannot be reached between all particles at the same time. Indeed, hexagonal order is very rare unless one restricts the area available to the system, bringing the particles so close together that the repulsive term dominates.

(v) Frustration for multiparticle interactions because of inadequate relative orientations must be the reason for the tendency towards the formation of linear aggregates [Fig. 3(a)(i)]. The increased interaction between particles at a domain boundary [the ''edge effect,'' Fig. 3(a)(ii)] is probably connected to frustration, as well, because fewer constraints have to be fulfilled at the boundary. This may have some relation with previous work on the fractal dimension of irregular colloidal aggregates at the water surface. Hurd and Schaefer [21] found a fractal dimension of 1.2 ± 0.15, which is less than what is expected from models of diffusion-limited aggregation [40]. These authors explicitly suggested an anisotropic interaction as the cause of this unexpected predominance of linear strings. Capillarity as described here may have also been of influence in these experiments.

Ideally, one would want to relate the two-particle interaction potential with the two-particle correlation function. Density-functional theory provides quantitative relations between those two quantities, which are, however, derived under certain approximations [41]. We did not attempt such a comparison for a number of reasons. Most importantly, the observation of the video tapes showed that the assembly of spheres is in a nonergodic state in the sense that the variations in the interparticle distance are frozen in. We searched for a transition between ergodic (''liquid'') and a nonergodic (''glassy'') states, but could not reach the liquidlike state. Clearly, the observed disorder is static and caused by the heterogeneity in the meniscus shape.

From inspection of the micrographs in Fig. 3, one can estimate that the width of the distribution of interparticle distances is somewhat less than the average interparticle distance. One could argue that this distribution is narrower than expected for a completely random distribution of meniscus irregularities. However, there is no direct relation between the minimum of the interparticle potential and the meniscus irregularity. Conversely, the distance of minimum interparticle energy may be given by the characteristic length where the approximations leading to Eq. (18) break down. This length should be comparable to the particle diameter. The meniscus irregularity will then affect the depth of the minimum, but only to a minor extent its location on the distance scale.

We do not claim that nonuniform wetting provides a complete explanation of all aspects of the interaction. There is a vivid debate concerning an attraction between like charges in aqueous solution [38], which certainly may have a connection to the attractive forces encountered here. However, the main experimental features are well accounted for by our explanation based on capillarity and nonuniform wetting. Particle interaction due to an irregular contact line explains the long-range nature of the forces as well as the cluster morphology. The same formalism applies to particles trapped at other fluid interfaces like liquid-liquid interfaces or the membranes of foams. A nonideal three-phase contact line will always introduce excess surface area and excess surface energy, and hence an attractive force. On these grounds, we believe that capillary forces originating from nonuniform wetting will be an essential ingredient to any model trying to describe particle interactions at fluid interfaces.

VI. CONCLUSIONS

We have described a mechanism for lateral attraction of colloidal particles at the air-water interface, based on an irregular shape of the meniscus and a concomitant distortion of the water surface. The macroscopic analog of this scenario is easily demonstrated by spreading corn flakes on a water surface. Surface tension rotates the individual flakes around and pulls them together to form strings and rafts. The quantitative calculation uses a multipole expansion, where the leading quadrupolar term results in a net attraction depending on the inverse fourth power of distance. For particle diameters of 1 μm, interparticle distances of 2 μm, and 50-nm deviations of the meniscus from the ideal straight line, we find potential wells with a depth of about $10^4 kT$.

To substantiate the hypothesis of a distorted contact line we modified the particle surface by addition and elution of detergent. The interaction reversibly depended on the detergent concentration, proving that capillarity is part of the explanation. Since the meniscus line is different for each particle there is a broad heterogeneity in the interparticle forces. The formation of hexagonal arrays is frustrated because the optimum orientation cannot be assumed between all interacting particles at the same time. Linear arrays are common for the same reason. This kind of capillary force should be of relevance for particles trapped at many kinds of fluid interfaces.

APPENDIX: INTERPARTICLE POTENTIAL UNDER NONUNIFORM WETTING CONDITIONS FOR VERY LOW INTERPARTICLE DISTANCE

The interaction potential at low particle distance is complicated, and depends on the relative strengths of the differ-

ent multipole orders, which are not known. However, the picture again simplifies when the distance between the particle surface $D(D=L-2r_c)$ becomes much smaller than both the radius r_c and the correlation length of the meniscus irregularities. Because the distance between the particle surfaces is the shortest length scale the field $h(x,y)$ locally interpolates between the conflicting boundary conditions, that is,

$$h(x,y)\approx\frac{1}{2}\left(1+\frac{x}{x_-(y)}\right)h(x_-(y),y)+\frac{1}{2}\left(1+\frac{x}{x_+(y)}\right)h(x_+(y),y),\tag{A1}$$

$$x_\pm(y)\approx\pm\left(\frac{D}{2}+\frac{y^2}{2r_c}\right).$$

For the definition of the variables, see Fig. 7(a). The excess area δS is given by

$$\begin{aligned}\delta S&\approx\int\frac{1}{2}(\nabla h)^2\,dx\,dy\\&\approx\tfrac{1}{2}\int_{-\infty}^{+\infty}(x_+(y)-x_-(y))\left[\frac{h(x_+(y),y)-h(x_-(y),y)}{x_+(y)-x_-(y)}\right]^2dy\\&=\tfrac{1}{2}\int_{-\infty}^{+\infty}\frac{[h(x_+(y),y)-h(x_-(y),y)]^2}{2\left(\frac{D}{2}+\frac{y^2}{2r_c}\right)}dy.\end{aligned}\tag{A2}$$

Assuming that the correlation length of the meniscus line is much smaller than the radius r_c one may replace $[h(x_+(y),y)-h(x_-(y),y)]^2$ by its average $\langle[h(x_+(y),y)-h(x_-(y),y)]^2\rangle:=\langle\Delta h^2\rangle$. The excess area becomes

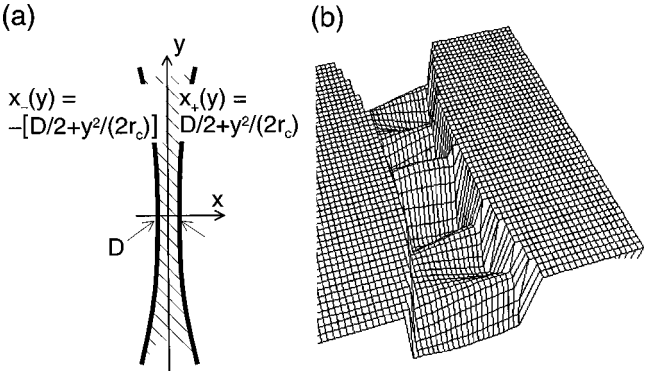

FIG. 7. Situation for a small gap D between the two spheres. (a) Definition of some variables. (b) Height of the water surface in the gap. For the purpose of illustration the meniscus lines have been chosen as two incommensurate cosines. If the shapes of the distorted contact lines are different on the two particles, a steep slope of the water surface in between the particles is unavoidable, at least at some places. The slope becomes steeper with decreasing particle distance, resulting in a repulsive force.

$$\delta S\approx\int_{-\infty}^{+\infty}\frac{\langle\Delta h^2\rangle}{4\left(\frac{D}{2}+\frac{y^2}{2r_c}\right)}dy=\langle\Delta h^2\rangle\left(\frac{\pi^2 r_c}{4D}\right)^{1/2}.\tag{A3}$$

The above calculation is limited to the gap area. Inside the gap, the excess area δS actually *increases* with decreasing distance, resulting in a repulsive force. Note that this increase may be compensated for by the area outside the gap. Also, it may safely be assumed that in reality the meniscus will slip if the boundary conditions are in conflict to the extent sketched in Fig. 7(b). We do not claim that there really is a repulsive force at small distances. The only point we want to make is that the capillary interaction levels off at small distances and certainly has a distance dependence weaker than L^{-3}. Provided that this is the case, the electrostatic dipole-dipole repulsion outweighs capillarity attraction at small distances and the particles remain at a finite distance, rather than aggregating into continuous rafts.

[1] K. Zahn and G. Maret, Curr. Opin. Colloid Interface Sci. **4**, 60 (1999).
[2] P. Pieranski, Phys. Rev. Lett. **45**, 569 (1980).
[3] K. Zahn, R. Lenke, and G. Maret, Phys. Rev. Lett. **82**, 2721 (1999).
[4] J. M. Kosterlitz and D. J. Thouless, J. Phys. C **6**, 1181 (1973).
[5] C. Duschl, D. Stamou, M. Liley, and H. Vogel, ACS Abstracts, *Proceedings of the 216th ACS National Meeting, Boston, August 1998* (American Chemical Society, Washington, D.C., 1998), Polymer Section, p. 500.
[6] F. Burmeister, W. Badowsky, T. Braun, S. Wieprich, J. Boneberg, and P. Leiderer, Appl. Surf. Sci. **145**, 461 (1999).
[7] J. H. Fendler, Curr. Opin. Colloid Interface Sci. **1**, 202 (1996).
[8] P. A. Kralchevsky, V. N. Paunov, I. B. Ivanov, and K. Nagayama, J. Colloid Interface Sci. **151**, 79 (1992).
[9] W. B. Russel, D. A. Saville, and W. R. Schowalter, *Colloidal Dispersions* (Cambridge University Press, Cambridge, England, 1989).
[10] A. W. Adamson and A. P. Gast, *Physical Chemistry of Surfaces*, 6th ed. (Wiley, New York, 1997), p. 510, and references therein.
[11] K. Shinoda and S. Friberg, *Emulsions and Solubilization* (Wiley, New York, 1986).
[12] J. Ruiz-Garcia, R. Gámez-Corrales, and B. I. Ivlev, Physica A **236**, 97 (1997).
[13] F. Ghezzi and J. C. Earnshaw, J. Phys. Condens. Matter **9**, L517 (1997).
[14] F. Ghezzi and J. C. Earnshaw, Nuovo Cimento D **20**, 2243 (1998).
[15] J. Ruiz-Garcia and B. I. Ivlev, Mol. Phys. **95**, 371 (1998).
[16] J. Ruiz-Garcia, R. Gámez-Corrales, and B. I. Ivlev, Phys. Rev. E **58**, 660 (1998).
[17] D. J. Robinson and J. C. Earnshaw, Langmuir **9**, 1436 (1993).
[18] R. Kesavamoorthy, C. B. Rao, and B. Raj, J. Phys.: Condens. Matter **5**, 8805 (1993).
[19] G. Y. Onada, Phys. Rev. Lett. **55**, 226 (1985).
[20] J. Stankiewicz, M. A. C. Vílchez, and R. H. J. Alvarez, Phys. Rev. E **47**, 2663 (1993).

[21] A. L. Hurd and D. W. Schaefer, Phys. Rev. Lett. **54**, 1043 (1985).
[22] J. N. Israelachvili, *Intermolecular and Surface Forces*, 2nd ed. (Academic, London, 1992).
[23] D. Y. C. Chan, J. D. Henry, and L. R. White, J. Colloid Interface Sci. **79**, 410 (1981). There is a typographical error in Eq. (43), where the factor g^2 (g the gravitational acceleration) is missing.
[24] P. A. Kralchevsky and K. Nagayama, Langmuir **10**, 23 (1994).
[25] G. S. Lazarov, N. D. Denkov, O. D. Velev, P. A. Kralchevsky, and K. Nagayama, J. Chem. Soc., Faraday Trans. **90**, 2077 (1994).
[26] Similar accounts of clustering behavior exist since 1997, and all are based on commercial products (Duke Scientific Corp., Molecular Probes, Polysciences Inc.) (Refs. [12] and [13]). Considering that people have been working with similar systems for more than five years (Ref. [17]), we find it remarkable that the phenomenon has not been reported earlier. Possibly, the occurence of clustering is related to changes in the particle production protocols (e.g., surfactant-free manufacturing) which may have resulted in altered surface properties.
[27] E. L. Decker and S. Garoff, Langmuir **13**, 6321 (1997).
[28] A. Y. Fadeev and T. J. McCarthy, Langmuir **15**, 3759 (1999).
[29] R. J. Good and E. D. J. Kotsidas, J. Colloid Interface Sci. **66**, 360 (1978).
[30] J. L. Rigaud, D. Levy, and G. Mosser, Eur. Biophys. J. **27**, 305 (1998).
[31] E. H. Mansfield, H. R. Sepangi, and E. A. Eastwood, Philos. Trans. R. Soc. London, Ser. A **355**, 869 (1997).
[32] N. D. Denkov, P. A. Kralchevsky, and I. B. Ivanov, J. Dispersion Sci. Technol. **18**, 577 (1997).
[33] M. A. Fortes, Can. J. Chem. **60**, 2889 (1982).
[34] A. W. Adamson and A. P. Gast, *Physical Chemistry of Surfaces* (Wiley, New York, 1997).
[35] Strictly speaking, in an environment with a nonvanishing gradient ∇h, the particle will adjust its polar axis such that the ''north pole'' is perpendicular to the gradient. Equivalently one could rotate the local coordinate system such that ∇h vanishes. Since gravity is neglected, the local z axis may be defined as being perpendicular to the water surface, whatever the local inclination of the water surface is. The *curvature* of the water surface interacting with the quadrupole moment *cannot* be transformed away by a rotation of the local coordinate system.
[36] See, for example, J. D. Jackson, *Electrodynamics* (de Gruyter, New York, 1983).
[37] A. J. Hurd, J. Phys. A **18**, L1055 (1985).
[38] A. E. Larsen and D. G. Grier, Nature (London) **385**, 230 (1997).
[39] R. W. Bowen and A. O. Shariff, Nature (London) **393**, 663 (1998).
[40] T. A. Witten, Jr. and L. M. Sander, Phys. Rev. Lett. **47**, 1400 (1981).
[41] See, for example, M. Plischke and B. Bergersen, *Equilibrium Statistical Physics*, 2nd ed. (World Scientific, Singapore, 1994).